Neural Comput & Applic
DOI 10.1007/s00521-016-2212-0

ORIGINAL ARTICLE

Preparation and optimization of chitosan/polyethylene oxide nanofiber diameter using artificial neural networks

Najmeh Ketabchi[1] · Majid Naghibzadeh[2] · Mahdi Adabi[1] · Seyedeh Sara Esnaashari[1] · Reza Faridi-Majidi[1]

Received: 17 March 2015 / Accepted: 19 January 2016

Abstract Chitosan/polyethylene oxide (PEO) solution makes electrospun nanofibers with decreased beads and diameters in comparison with lonely chitosan (CS). The aim of this work was to find an artificial neural network (ANN) model for predicting the chitosan/PEO blend electrospun nanofiber diameter. Chitosan/PEO concentration ratio, distance between nozzle tip and collector, applied voltage, and flow rate were considered as input variables, and chitosan/PEO blend electrospun nanofiber diameter was considered as output variable. Scanning electron microscopy images indicated that electrospun nanofiber diameter was approximately 50–185 nm. For increasing validity, *k*-fold cross validation method was applied to dataset. The ANN technique was used for training and testing via fivefold of dataset. The best results of prediction were obtained via network with three hidden layers including 10, 15, and 5 nodes in each layer, respectively. The mean square error (MSE) and correlation coefficient between the observed and predicted thickness of the nanofibers in the chosen model were about 0.0707 and 0.9630, respectively, indicating the ANN technique validity in the prediction procedure. For the analysis of interactions between the involved electrospinning parameters and nanofiber diameter, 3D graphs in various levels were plotted. In conclusion, the results indicated that using the prediction process via ANN could be relevant in the decision to produce nanofibers with desired shape and diameter via electrospinning.

Keywords Chitosan · Polyethylene oxide · Electrospinning · Nanofibers · Modeling · ANN

1 Introduction

Nanofibers have attracted great attention owing to their advanced properties such as high surface area [1–8], high porosity [1–5, 7], flexibility in surface functionalities [3, 5, 6], small diameter [7, 8], and superior mechanical performance (e.g., stiffness and tensile strength) [3, 5, 9]. They are generally defined as fibers <1 μm in size which have great potential in the various fields such as filtration membranes [1–7, 10], electrical and optical applications [5, 7, 8], energy harvest and storage (e.g., solar cells, fuel cells, lithium ion batteries) [2, 7], cosmetics [3], and biomedical applications [2, 4].

Nanofibers are made by a variety of methods, such as melt blowing [5, 11], drawing, template synthesis [5, 12], wet and dry spinning [8, 12], phase separation [5, 12, 13], self-assembly, and electrospinning [5, 11–13]. But electrospinning seems a more versatile method to fabricate nanofibers from polymer solutions for a broad set of polymeric materials with a relatively high velocity, simplicity, efficiency, and controllability over the diameter and orientation of the fibers [3, 14]. Furthermore, it is just a method for the synthesis of one-by-one single continuous nanofibers with a board range in fiber diameter from 3 nm

Electronic supplementary material The online version of this article (doi:10.1007/s00521-016-2212-0) contains supplementary material, which is available to authorized users.

✉ Reza Faridi-Majidi
refaridi@tums.ac.ir

[1] Department of Medical Nanotechnology, School of Advanced Technologies in Medicine, Tehran University of Medical Sciences (TUMS), Tehran, Iran

[2] Department of Nanotechnology, Research and Clinical Center for Infertility, Shahid Sadoughi University of Medical Sciences, Yazd, Iran

Published online: 19 February 2016

to >5 μm on a large amount of variety of materials [5, 10, 15]. Electrospinning technically works in a high electric field to fabricate fine filaments from the polymer solution [2]. The typical setup consists mainly of a syringe pump, a needle nozzle, a collector drum, and high-voltage-power source [2, 10]. During the electrospinning process, the polymer solution was filled in a syringe pump. When the device turns on, the polymer solution is ejected from a steel needle and a jet is created. Afterward, a high-voltage source is applied to draw the fluid into a liquid jet, so the jet travels from the needle to the rotating collector [3, 6].

The diameter of nanofibers affects the surface area and pores. Therefore, the specific usage of nanofibers such as membranes or scaffolds requires a given diameter [8, 13, 16–20]. But to achieve desired diameter, levels of experiment are very complex and fabrication of electrospun nanofibers with preferred diameters would be expensive and time-consuming process. Researchers have tried to find a scientific model with prediction capability of patterns in various processes [11, 14, 21]. Nowadays, there are some data mining processes that are reliable to predict significant relationship between data using effective techniques such as response surface methodology (RSM), Box–Benkhen design (BBD), and ANN techniques [11, 17, 22].

The most applied methods for the prediction of nanofiber diameter are RSM and ANN. ANN and RSM are mathematically two powerful methods using modeling and simulation of a number of processes in real applications, especially in modeling electrospinning process for the prediction of nanofiber diameter [22–25]. During the last two decades, ANN, a nonlinear multivariate modeling, has emerged and developed using predictive tool. Indeed, the specific structure and the ability to learn based on the available data are considered as the attraction of ANNs. On the other hand, RSM is an experimental and statistical technique for modeling multiple regression analysis. In this method, quantitative data obtained from well-designed tests are used for solving multivariate equations at the same time [26]. However, there are similarities and differences in using two attractive methods, ANN and RSM, for modeling and predicting procedures. The main advantage of ANN in comparison with RSM includes the lack of need to a prior specification of appropriate fitting function via ANN and its widespread estimation capabilities, whereas RSM is a convenient method only for quadratic approximations [26]. It seems that ANN needs more number of experiments than RSM to build an effective mode; however, practically ANN works well even with comparatively less data and pattern, if the data are statistically well distributed in the training process and inputs, which is the case with design of experiment. Therefore, it seems that the trial data of RSM should be adequate for designing an effective ANN model. Of course, in some literature, ANN models indicated better performance in comparison with RSM [27, 28]. However, RSM, based on its structured nature, is more valuable in getting insight information (i.e., sensitivity analysis and interactive outcome of two components on the system) than ANN. Nevertheless, there are similarities between ANN and RSM as modeling method, such as the lack of need to the explicit expressions of the physical meaning of the system or process under investigation, and dealing with the development of nonparametric simulative models [29]. In addition, the functional associations between independent variables and the response of the modeling process are approximated by these methods using trial data. Subsequently, the designed models could be saved and used as an estimation method for the optimal setting of independent variables to reduce errors and correct the responses [30].

ANN, a computational method with nonlinear mapping structure, takes different units in the input and output layer, based on the human neural network [31, 32]. It consists of several units interconnected together for discovering relationships between them and estimating relevant outputs [11]. The modeling is based on transferring function into the output at specific algorithm using sophisticated data search programmed in functions [11, 33, 34]. ANNs can be used to extract patterns and detect trends which are too complex to be noticed by either humans or other computer techniques [31]. Nowadays, various ANN models and learning algorithms have been recognized for a large variety of classification and prediction patterns. In various scientific and industrial fields, such as space, traffic, banking, electronics, and medicine, therefore, it has been successfully known as a descriptive method in all unknown parameters. Nevertheless, despite the several benefits of ANN such as the ability to learn and adaptive learning to solve the complex problems, there are some known limitations using ANN including its "black box" nature, the proneness of over fitting, and the empirical nature of model development [35].

As yet, there have been many studies with this approach, and there are so many models that are predicted with ANN device. For example, Maleki et al. [7] predicted release profile of tetracycline hydrochloride from polymeric core shell electrospun nanofibers via ANN method. Aghajani et al. [36] investigated major factors affecting the stability of an acetaminophen nanosuspension through nanoprecipitation in microfluidic reactors using ANN model. The tensile moduli of carbon nanofiber (CNF)/epoxy composites were predicted via ANN by Chen [37]. Adabi et al. [38] studied parameters affecting carbon nanofiber electrodes for measurement of the cathodic current in the electrochemical sensors using ANN. These demonstrate the increasing interest, importance, and success of ANN-based modeling in this area of research.

Chitosan, a natural polymer produced by the hydrolysis of chitin, is useful in wound-healing and antimicrobial scaffolds. Besides, it is biocompatible and biodegradable in human body [39–41]. But it is difficult to produce electrospun nanofibers due to its high surface tension and high viscosity in solution [39–41], because it produces beaded and short noncontinues fibers. To overcome these difficulties, chitosan can be used by blending with other biocompatible and biodegradable polymers, such as PVA [42] and PEO, for the biomedical applications [40]. To our knowledge, the prediction of chitosan/PEO blend electrospun nanofiber diameter has not been studied by ANN modeling yet. In this paper, to prepare chitosan/PEO nanofibers, four parameters involved in electrospinning (chitosan/PEO concentration ratio, applied voltage, flow rate, and distance between nozzle tip and collector) were considered as variable parameters, and the validity of ANN models for the prediction of nanofiber diameter was formulated.

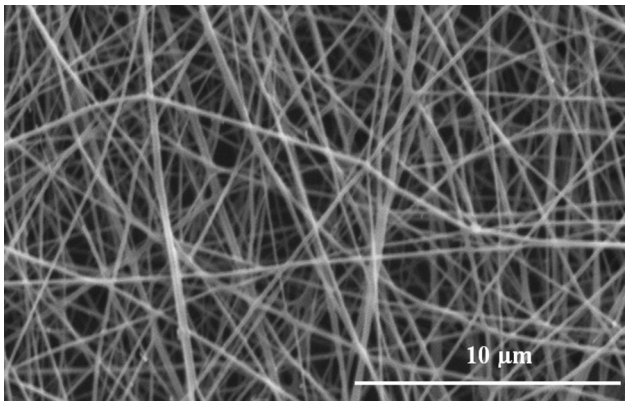

Fig. 1 SEM image of electrospun chitosan/PEO nanofibers

2 Materials and methods

In this work, chitosan (low molecular weight: 2.5 KD, Easter group (Dong Chen Co. Ltd) and PEO (MW 900KD, Acros Organics) were used as polymers, and glacial acetic acid (AcOH, Merck Chemical) was used as solvent. The polymer solution blend was electrospun into nanofibers using Electroris (FNM Ltd., Iran, www.fnm.ir) as an electrospinning instrument.

2.1 Methods

Four independent parameters were chitosan/PEO concentration ratio, applied voltage, distance between nozzle tip and covered collector with aluminum plate, and flow rate, during the study. All samples were sputtered with gold, and then, images were taken using SEM. Afterward, the diameter of random 40 fibers was measured and considered as the mean diameter of the fibers for each sample (Fig. 1). As the diameter of nanofibers was not uniform, we measured 40 nanofiber diameter for each sample to diminish the errors. Therefore, the errors were negligible.

2.2 Artificial neural network modeling

The prediction of the nanofiber diameter was performed via an ANN with different hidden layers and nodes, and the accuracy of these predictions was evaluated by MATLAB software. Based on previous works, the *k*-fold cross validation method was used to obtain better results. In this study, the back-propagation (BP) feed forward network with Levenberg–Marquardt learning algorithm is employed. The BP networks are one of the common methods for training ANNs in conjunction with an optimization method such as

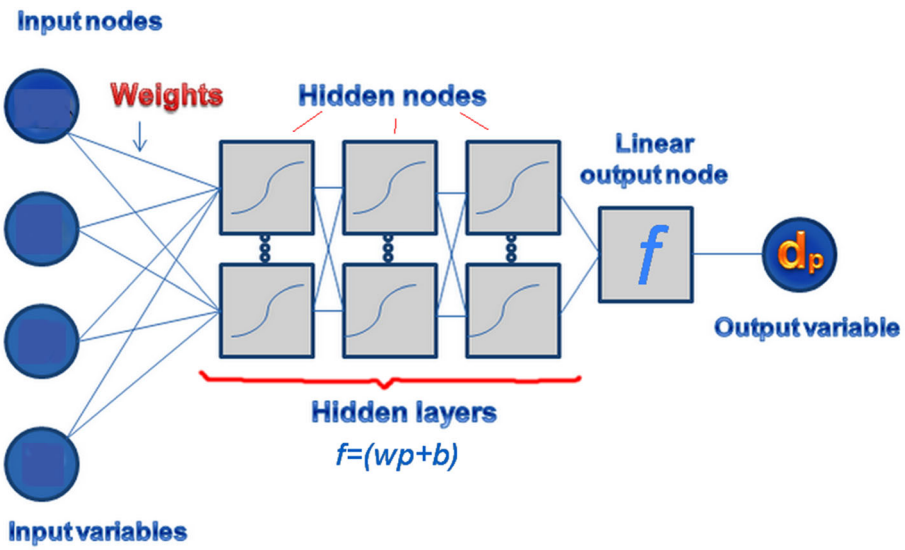

Fig. 2 Schematic of the architecture of BP networks

gradient descent that the gradient of a loss function is calculated by method with respect to all the weights in the network. For minimizing the function loss, the gradient is fed to the optimized method for updating the weights. The most common architecture of BP networks, multilayer feed forward networks, is schematically shown in Fig. 2.

Three different layers, input layer, hidden layers, and output layer, have formed the BP networks. For designing the relevant network, the number of each layer could be estimated via testing the accuracy of the network in prediction outputs. The weights of the neurons for regulating the network response could be applied automatically via selected network before and during the training process.

Mathematically, a neuron of an ANN (*m*) could be characterized based on the following equations [43].

$$r_m = \sum_{i=1}^{n} (w_{mi} x_i + b_m) \quad (1)$$

$$y_m = f(r_m) \quad (2)$$

where x_1, x_2,…,x_n specify the input signals; w_{m1}, w_{m2}, …, w_{mn} are the neuron synaptic weights; b_m is the bias; y_m is the neuron's output signal; f is the activation function; and r_m is the linear combiner output [43].

One of the main drawbacks of ANNs is their unknown process for attribution of weights to inputs. Due to the numbers of the parameters and using new function on feed forward network in this study, 250 weights were attributed automatically (based on the three hidden layers with 10, 15, and 5 nodes, respectively). Therefore, it seems that referring to the impressive number of weights in the text might be illogical and unusual.

2.3 Network models designed for prediction

Various sets of electrospinning experiments were designed based on different values of four effective variables, including chitosan/PEO concentration ratio (X1) (w/w), applied voltage (X2) (kV), distance (X3) (cm), and flow rate (X4) (ml/h) (Table 1).

Data are categorized into two groups: training and testing group. The training group is used for adjusting the network weights, whereas testing group is applied to assess the efficiency of the network. Previous studies have shown that simple dataset is not practical for the prediction via ANN when the database is small, while with a large database, the efficiency of the ANN model may not be reliable to use for the estimation of future samples if a simple training–test dataset dividing procedure is used. Instead, *k*-fold cross validation method is used and leads to less bias than the simple training–test dataset dividing process. The *k* equal subsets (Table 2) of database were randomly partitioned into the two main categories, testing and training set. The function of approximation is repeated

Table 1 List of input variable for electrospinning

Independent input variable	Description
X_1	Chitosan/PEO concentration ratio (w/w)
X_2	Applied voltage (kV)
X_3	Distance (cm)
X_4	Flow rate (ml/h)

Table 2 Training–testing partition pairs using tenfold cross validation method

Partition pairs	Training set	Testing set
1	Partition {1,2,3,4,5,6,7,8,9}	Partition {10}
2	Partition {1,2,3,4,5,6,7,8,10}	Partition {9}
3	Partition {1,2,3,4,5,6,7,9,10}	Partition {8}
4	Partition {1,2,3,4,5,6,8,9,10}	Partition {7}
5	Partition {1,2,3,4,5,7,8,9,10}	Partition {6}
6	Partition {1,2,3,4,6,7,8,9,10}	Partition {5}
7	Partition {1,2,3,5,6,7,8,9,10}	Partition {4}
8	Partition {1,2,4,5,6,7,8,9,10}	Partition {3}
9	Partition {1,3,4,5,6,7,8,9,10}	Partition {2}
10	Partition {2,3,4,5,6,7,8,9,10}	Partition {1}

k times to fit function via training dataset, as $k - 1$ subsets are put from a training set and remaining subset is also used as the test set.

2.4 Network training using *k*-fold cross validation procedure

Forty electrospun nanofiber samples were prepared through the electrospinning process and applied as ANN models training–testing dataset. As shown in Table 3, beaded nanofibers are formed in the seven experiments (8, 24, 25, 26, 27, 28, 29). But all of 40 samples were used in practice to train and test the ANN models.

Data normalization was performed before using ANN modeling.

The data normalization Eq. (3):

$$y_{\text{norm}} = (y_{\max} - y_{\min})(x - x_{\min})/(x_{\max} - x_{\min}) + y_{\min} \quad (3)$$

where $y_{\min}$ and $y_{\max}$ are equal to -1 and 1, respectively. X = the data that should be normalized.

$x_{\max}$ = the maximum values of x

$x_{\min}$ = the minimum values of x

The training setting parameters for ANN modeling are shown in Table 4.

2.5 ANN models training

In the following, six models of neural networks were designed with various structures, including four units

Table 3 Training dataset for ANNs modeling

Sample no	Chitosan/ PEO	Applied voltage (Kv)	Distance (mm)	Device rate	Comment	Observed diameter (nm)	Predicted diameter (nm)
1	9	20	70	1		86.5	78.2
2	9	23.1	80	1		83.5	78.2
3	9	20	90	1		76.9	78.2
4	9	24.1	70	0.8		84.5	78.2
5	9	24.7	80	0.8		80.7	76
6	9	24.3	90	0.8		82.8	76
7	9	20	70	0.5		74.5	71.5
8	9	26	100	0.5	Beads + nanofibers	70.5	71.5
9	4	20	70	1		108.	111
10	4	21.5	90	1		135.5	120
11	4	21.8	100	1		169.5	132.7
12	4	21.5	70	0.8		132.8	112.6
13	4	21.6	80	0.8		142.5	114
14	4	21.2	90	0.8		172	179.9
15	4	21.2	100	0.8		183.5	184
16	4	21.4	70	1.5		82	67.5
17	4	21.3	80	1.5		95	87
18	4	21.6	90	1.5		78.5	79
19	4	21.6	100	1.5		84.5	81
20	4	22.1	70	1.2		77	79.5
21	4	21.3	80	1.2		73.7	75.5
22	4	21.2	90	1.2		71.8	73.5
23	4	21.2	100	1.2		89.5	96
24	9	25	70	1	Beads + nanofibers	81.06	76.5
25	9	21.1	80	1	Beads + nanofibers	92.06	86
26	9	22	90	1	Beads + nanofibers	101.04	87
27	9	20	100	1	Beads + nanofibers	84.02	73.5
28	9	20	70	0.5	Beads + nanofibers	60.8	68.5
29	9	20	70	0.8	Beads + nanofibers	70.4	71.8
30	9	20	80	0.8		71.8	71.8
31	9	22.7	90	0.8		71.9	71.8
32	9	22.4	70	1.5		78.44	72.5
33	9	22.6	80	1.5		81	75.5
34	9	22.5	70	1.2		73.7	57.6
35	4	21	70	0.5		86.76	85.4
36	4	23.2	80	0.5		51.88	31.8
37	4	23.5	90	0.5		63.5	62.4
38	4	23.5	100	0.5		67.4	62
39	4	21	70	1		96.04	76.9
40	4	23.5	80	1		68	64.6

in the input layer, one unit in output layer, and various hidden layers with different nodes. When the network architecture completed, training dataset was used to train the network and then tested with testing data.

3 Results and discussion

In Table 5, the mean square error and correlation coefficient (R) of the test dataset obtained from the selected ANN model are shown.

Table 4 ANN training parameters

Algorithm = trainlm (Levenberg–Marquardt back-propagation)
Transfer function in hidden layers = log-sigmoid and purelin
Number of epochs between showing the progress = 50
Learning rate = 0.09
Momentum constant = 0.9
Maximum number of epochs to train = 1000
Performance goal = 1e−5

Table 5 Mean square error and linear regression of the tests data

ANN network $_{(10\ 20\ 5\ 1)}$	Mse	*R*
1	0.0179	0.9869
2	0.0222	0.9863
3	0.0687	0.9803
4	0.0538	0.9615
5	0.1431	0.9187
6	0.0821	0.9622
7	0.0424	0.9714
8	0.1105	0.9356
9	0.1041	0.9580
10	0.0626	0.9690
Mean ± STD	0.0707 ± 0.039	0.9630 ± .0217

The number of hidden layers = 3

The nodes in each layer = 10, 15, and 5, respectively.

Mean square prediction error (MSPE) is given by Eq. (4):

$$\mathrm{MSPE}n = \frac{100}{Nte\sigma_{dn}^2}\sum_{i=1}^{Nte}(d_n(i) - d_{pn}(i))^2, n = 1, \ldots, 5 \qquad (4)$$

d_n = the observed nanofiber diameter

d_{pn} = the predicted diameter of nanofibers

n = the network number

Nte = the numbers of samples used for network testing

σ_{dn}^2 = the variance of d_n.

The analysis of the observed and predicted average fibers diameter and standard deviation was done through SPSS software (version 17).

Figure 3 depicts the linear regression between the observed and predicted diameter of the fibers.

The results indicated that the difference between observed and predicted mean of chitosan/PEO nanofiber diameters was about 6 nm (as shown in Table 6).

The Pearson's correlation coefficient between observed and predicted fiber diameter was obtained equal to 0.950 that is significant at the 0.01 % level (Table 7). To check the assumption that the residuals or error terms are normally distributed, the normal p–p plot of regression standardized residual of the study is shown in Fig. 4.

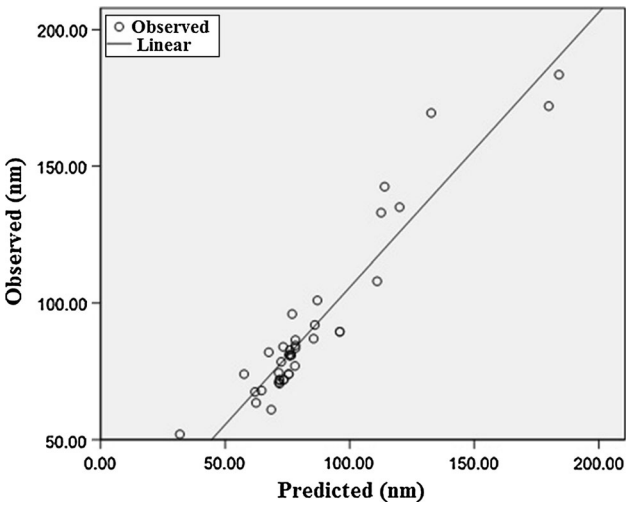

Fig. 3 Linear regression plot between observed and predicted diameters

Table 6 Descriptive statistics of the observed and predicted diameter

	Descriptive statistics				
	N	Minimum	Maximum	Mean	SD
Observed	40	52.00	183.50	90.4725	30.71711
Predicted	40	31.80	184.00	84.7850	28.96524
Valid *N* (listwise)	40				

Table 7 Correlation between the observed and predicted nanofiber diameter via ANN

Correlations	Observed	Predicted
Observed		
Pearson correlation	1	0.950**
Sig. (two-tailed)		0.000
Sum of squares and cross products	36,585.110	32,694.841
Covariance	938.080	838.329
N	40	40
Predicted		
Pearson correlation	0.950**	1
Sig. (two-tailed)	0.000	
Sum of squares and cross products	32,694.841	32,386.891
Covariance	838.329	830.433
N	40	40

** Correlation is significant at the 0.01 level (two-tailed)

Based on the results, the plot of residuals fits the expected pattern well enough to support a conclusion that the residuals are normally distributed. Taking into account

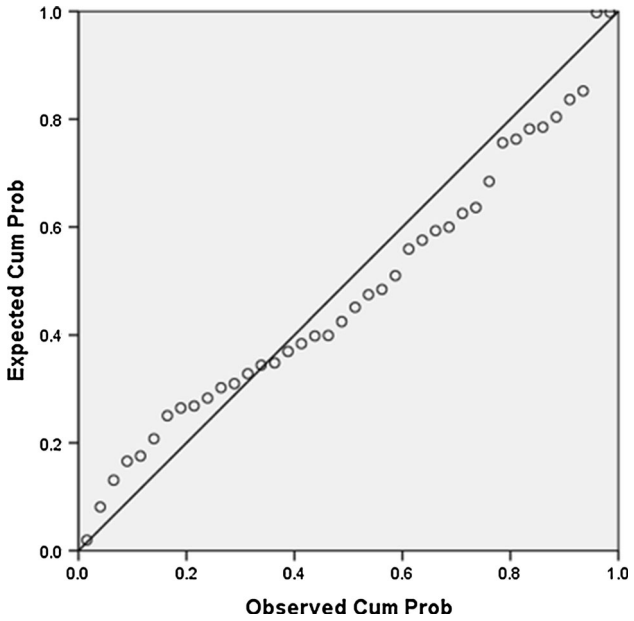

Fig. 4 Normal p–p plot of regression standardized residual

that relations between the processing conditions and the diameter of the electrospun nanofibers have very high degrees of complexity, these values indicate a satisfactory trained model.

Finally, the selected network was saved as a definite net in MATLAB software for future prediction of the other range of parameters based on the target. However, the network was tested using prediction of nanofiber diameter in out of range of variables. In addition, new relevant network should inevitably be designed and tried if the results were not satisfactory for study.

The Pearson's correlation coefficients (r) between the observed (d_n) and predicted (d_{pn}) nanofiber diameter are given in Eq. (5)

$$r = \frac{n(\sum d_n d_{pn}) - (\sum d_n)(\sum d_{pn})}{\sqrt{[n(\sum d_n^2) - (\sum d_n)^2][n\sum d_{pn}^2) - (\sum d_{pn})^2]}} \quad (5)$$

n = number of data.

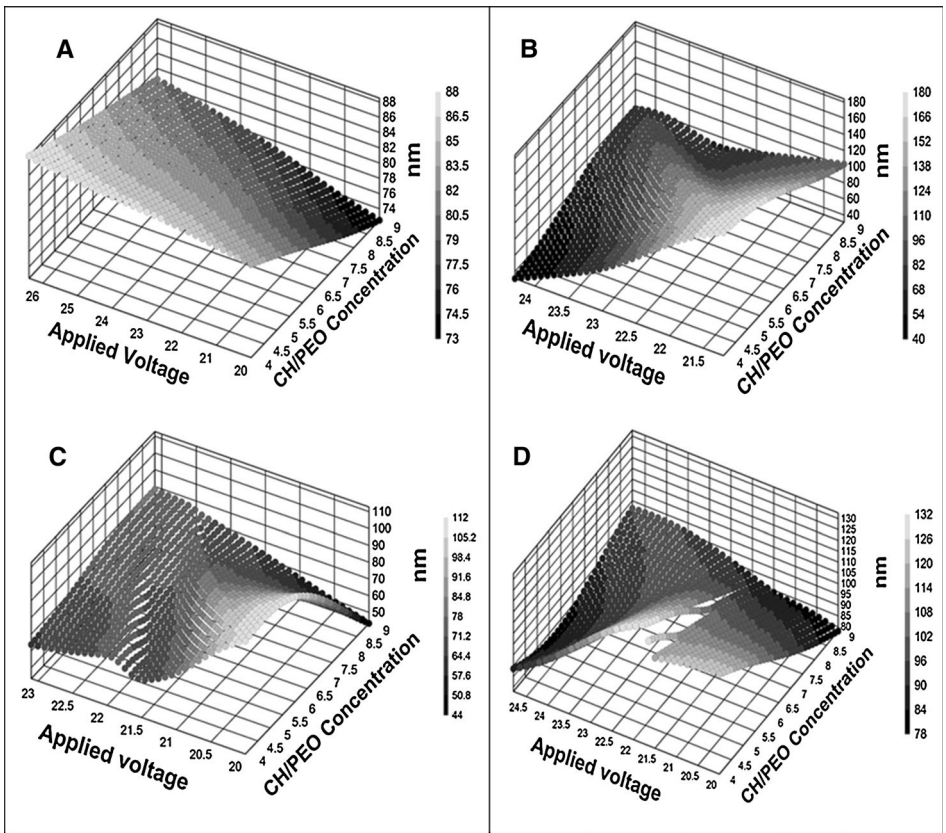

Diagrams \ Nanofibers diameter (Z) Data	Minimum Z (nm)	Maximum Z (nm)	Mean (nm)	Standard deviation
plot A, Low flow rate - nozzle to collector distance levels	72.5	88.5	81.7	3.45
plot B , Low flow rate - High nozzle to collector distance	62	184	98.45	57.33
plot C, High flow rate - Low nozzle to collector distance	67.5	111	79.55	15.81
plot D , High flow rate - nozzle to collector distance	78	132.7	101.2	23.70

Flow rate (ml/h) Levels= Low (0.5-0.99 ml/h), High (1-1.5 ml/h), Nozzle to collector distance (mm) Levels= High (90-100 mm), Low (70-89 mm)

Fig. 5 3D plots of applied voltage–polymer concentration, and data of nanofiber diameter modeling via ANN in different nozzle-to-collector distance and flow rate levels

3.1 3D plots patterns predicted the effect of input variables on the nanofiber diameters

As shown in the supplementary data, Table S1 indicates that 13.8 % of the changes in nanofiber diameter are dependent on the change in the applied parameters. The results of the change in chitosan/PEO concentration and applied voltage on nanofiber diameter are shown in Fig. 5. The minimum size of the fibers (mean diameter = 79.55 nm) was seen in the high flow rate–low distance between nozzle to collector (high R–low D level), while the maximum size was related to the high R–D level with 101.2 nm. The 3D plots (Fig. 5) also show that the fiber diameter decreases by increasing the chitosan/PEO concentration. The literature confirms that increasing concentration leads to increase in nanofiber diameter [44, 45]. This can be attributed to increase in viscosity and results in more resistant polymer solution and consequently thicker nanofibers. Table S2 indicates that 9.2 % of the changes in nanofiber diameter is dependent on the polymer concentration ($Pv < 0.05$). Table S3 demonstrates that the amount of nanofiber diameter enhances to 3.871 units as the polymer concentration increases one unit ($Pv < 0.05$). In addition, an inverse relationship was seen between the applied voltage and fiber diameter except in plot A which is in the low R–D range. It may be attributed to applied voltage which induces a higher electrical force and causes jet elongation and finally thinner nanofibers [44]. Table S4 indicates that 3.2 % of the changes in nanofiber diameter are dependent on the change in voltage ($P_V > 0.05$).

In Fig. 6, the effect of alteration in flow rate and chitosan/PEO concentration on fiber diameter in defined levels of applied voltage and distance from nozzle to the collector is investigated. The minimum fibers were produced in high V–low D with a mean diameter of 67.37 nm, while the maximum size is about 100.2 nm in low V–high D level.

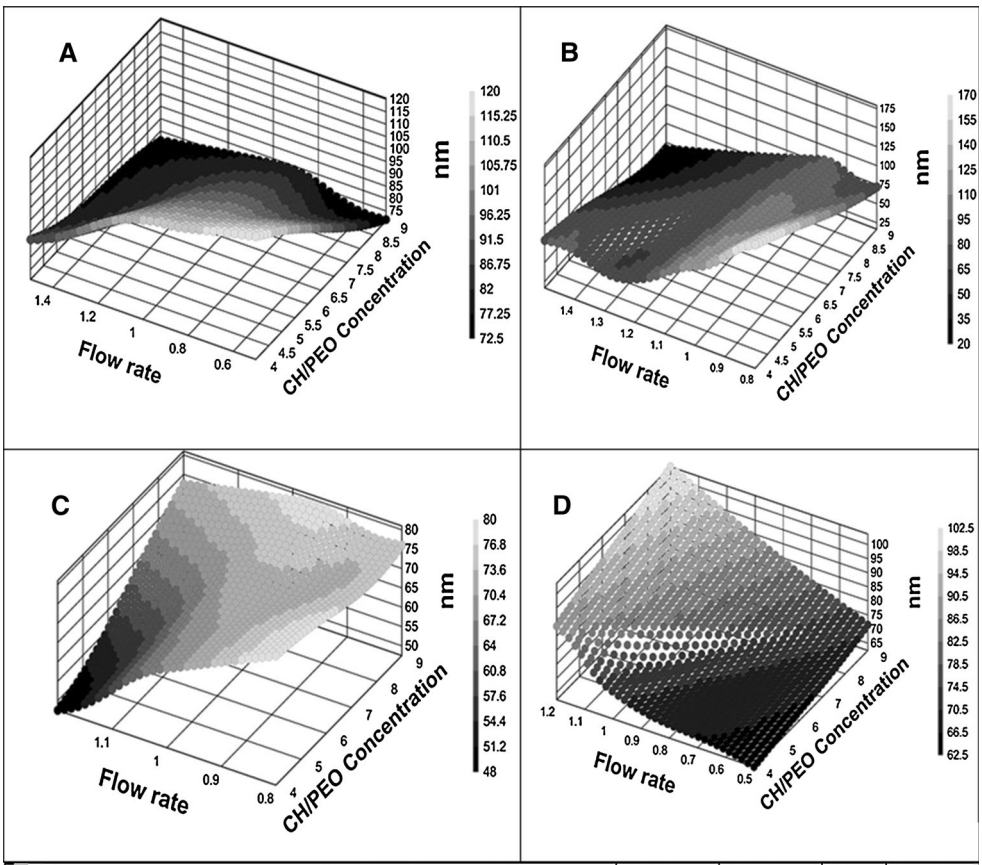

Diagrams \ Nanofibers diameter (Z) Data	Minimum Z (nm)	Maximum Z (nm)	Mean (nm)	Standard deviation
plot A, Low applied voltage & nozzle to collector distance levels	71.5	114	92.3	19.27
plot B , Low applied voltage -High nozzle to collector distance	71.8	179	100.2	42.57
plot C, High applied voltage -Low nozzle to collector distance	47.5	78	67.37	13.93
plot D , High applied voltage & nozzle to collector distance	62.4	88.5	73.6	10.87

Applied voltage (kV) Levels= Low (20-22.9 kV), High (23-26.5 kV),
Nozzle to collector distance (mm) Levels= High (90-100 mm), Low (70-89 mm)

Fig. 6 3D plots of polymer concentration–flow rate diagrams and data of nanofiber diameter modeling via ANN in different applied voltage and nozzle collector distance levels

On the other hand, by increasing applied voltage, thinner fibers were obtained while higher distance produced larger fibers. As shown in 3D plots, the flow rate inversely affects the fiber diameter except in the high V–D region, which can be the result of interaction between these parameters in this range. The effect of flow rate is contradictory to the nanofiber diameter. The literature shows that increase in flow rate of polymer solution can enhance the nanofiber diameter [44], whereas in some reports, there is a reverse relationship to the nanofiber diameter [21]. The reason for this reverse relationship may be attributed to the solvent which is evaporated at a low injection rate in comparison with high ones, resulting in an increase in concentration of the solution and consequently larger nanofiber diameter [46]. Table S5 indicates that the changes in nanofiber diameter are not dependent on the flow rate. The effect of chitosan/PEO concentration on fiber diameter is consistent with the 3D plots of Fig. 5.

The influence of fluctuation in the distance and chitosan/PEO concentration is simultaneously presented in Fig. 7 in specific regions of applied voltage and flow rate. The minimum average fiber size was about 67 nm achieved in high V–low R levels (plot C), and the maximum size was about 108 nm in low V–R domain. Moreover, applied voltage and flow rate both inversely affect the fiber diameter. It means that fiber size has descending and ascending trend as these two parameters increase and decrease, respectively. 3D plots in Fig. 7 present the direct relation between distance and fiber size. However, this trend was not seen in the low V–high R levels. Table S6 indicates that 5.6 % of the changes in nanofiber diameter is dependent on the distance changes in nozzle to collector ($P_V > 0.05$). The data in the literature also indicate that the effect of tip-to-collector distance on nanofiber diameter was not as much significant as other parameters [44]. The chitosan/PEO concentration shows inverse relation with fiber size in

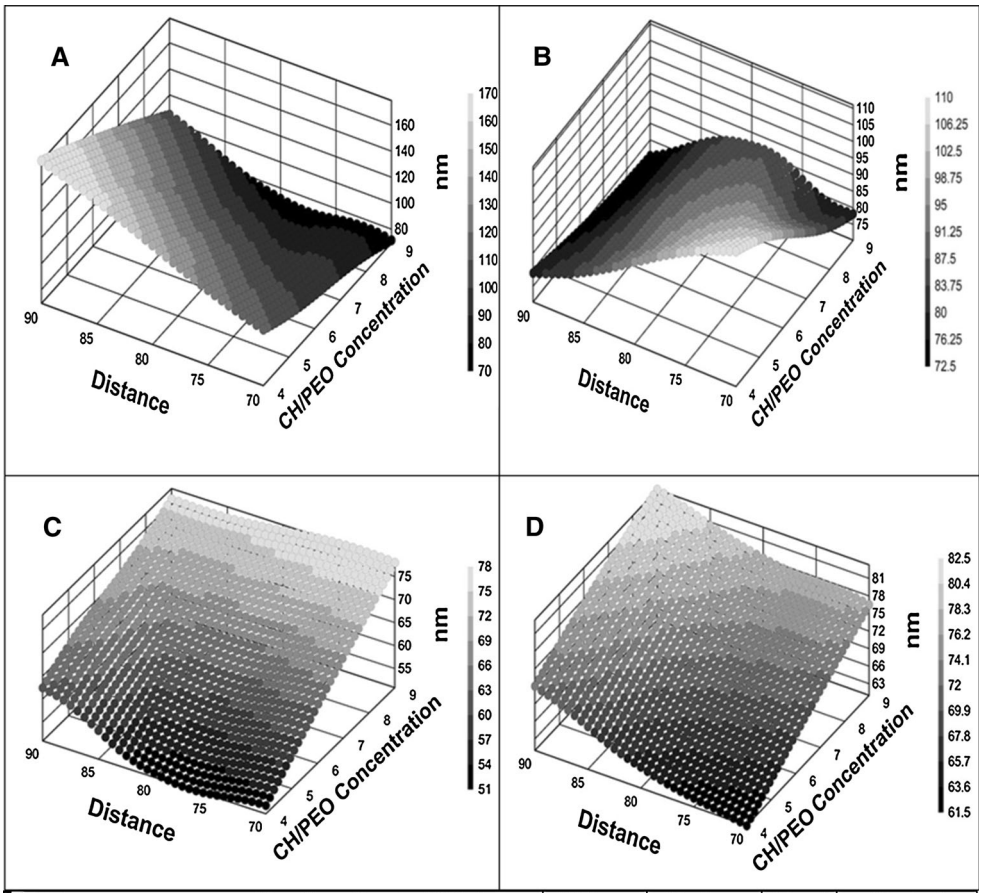

Diagrams \ Nanofibers diameter (Z) Data	Minimum Z (nm)	Maximum Z (nm)	Mean(nm)	Standard deviation
plot A, Low applied voltage & Flow rate levels	71.5	179	108.7	50.67
plot B , Low applied voltage - High Flow rate	78.2	111	88.85	15.37
plot C, High applied voltage -Low Flow rate	51.8	78	67.05	12.30
plot D , High applied voltage & Flow rate	64.6	78	72.77	6.01

Applied voltage (kV) Levels= Low (20-22.9 kV), High (23-26.5 kV), Flow rate (ml/h) Levels= Low (0.5-0.99 ml/h), High (1-1.5 ml/h),

Fig. 7 3D plots of polymer concentration–nozzle-to-collector distance, and data of nanofiber diameter modeling via ANN in different applied voltage and flow rate levels

plots A and B, while in plots B and C, increasing the chitosan/PEO concentration increased the fiber diameter. These two different trends happened in the low and high applied voltage regions. Hence, this dual behavior can be the effect of interaction between the voltage and chitosan/PEO concentration on the fiber diameter.

As listed in Fig. 8, the minimum and the maximum mean fiber diameters were approximately 75 and 99 nm, respectively. Moreover, fiber diameter shows an inverse relationship with both nozzle-to-collector distance and chitosan/PEO concentration. 3D plots illustrate that fiber diameter decreases as the flow rate and applied voltage decrease. But this direct relation is not observed in plot A. This inconsistency in plot A can be due to the interaction between flow rate and applied voltage in the low C–D region.

In order to evaluate the effect of applied voltage and nozzle-to-collector distance on fiber diameter, the flow rate and chitosan/PEO concentration were fixed in the determined range. The minimum size of the fibers was reported in high C–low R area (about 73 nm) and the maximum size was in the low C–R region (about 105 nm). As reported before, chitosan/PEO concentration has an inverse relation with fiber diameter. However, fiber size shows downward trend as flow rate increased as shown in Fig. 9. From the 3D plots, it is observed that higher applied voltage produces smaller fibers (with exception in high C–low R area). On the contrary, larger fibers were formed in higher distance between the nozzle and collector. However, this trend was not seen in the high C–low R area, again.

The plots of distance and flow rate against fiber diameter are depicted in Fig. 10 at a specific range of chitosan/PEO concentration and applied voltage. The largest and smallest mean fiber sizes were about 109 and 62 nm, respectively. Furthermore, the influence of the applied voltage and

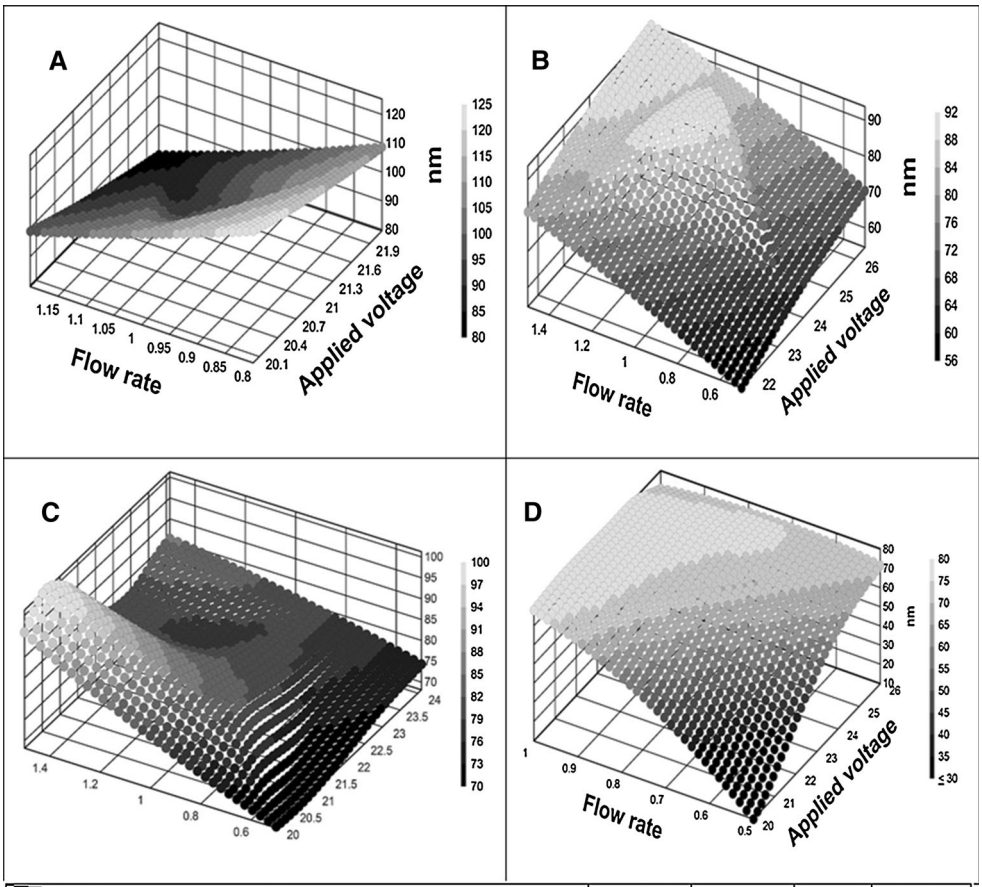

Diagrams \ Nanofibers diameter (Z) Data	Minimum Z (nm)	Maximum Z (nm)	Mean (nm)	Standard deviation
plot A, Low polymer concentration & nozzles to collector distance levels	79.5	112.6	99.77	15.44
plot B, Low polymer concentration -High nozzles to collector distance	62.4	88.56	79.99	12.22
plot C, High polymer concentration -Low nozzles to collector distance	68.5	86	78.42	7.36
plot D, High polymer concentration & nozzles to collector distance	71.5	87	75.95	7.41

Polymer concentration ratio Levels= Low (4-6.4), High (6.5-9),
Nozzle to collector distance (mm) Levels= High (90-100 mm), Low (70-89 mm)

Fig. 8 3D plots of applied voltage–flow rate, and data of nanofiber diameter modeling via ANN in different polymer concentration and nozzle-to-collector levels

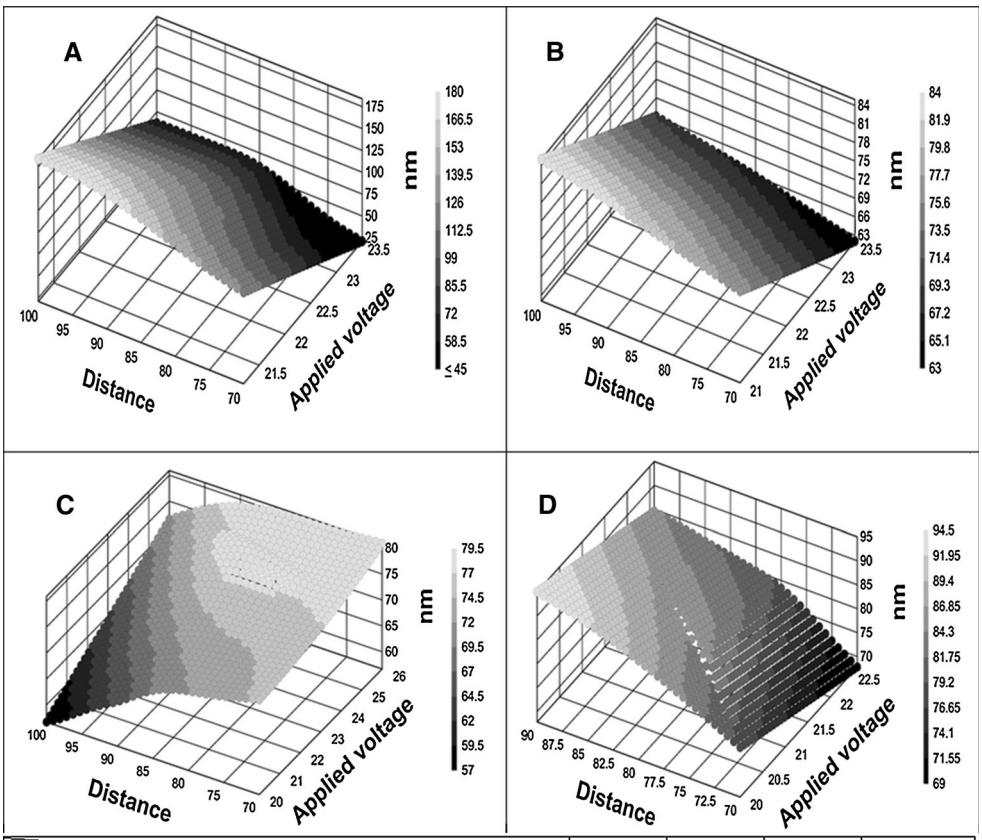

Fig. 9 3D plots of applied voltage–nozzle-to-collector distance, and data of nanofiber diameter modeling via ANN in different polymer concentration and flow rate levels

Diagrams \ Nanofibers diameter (Z) Data	Minimum Z (nm)	Maximum Z (nm)	Mean(nm)	Standard deviation
plot A, Low polymer concentration & Flow rate levels	62	184	105.25	57.6
plot B , Low polymer concentration - High Flow rate	64.6	81	75.37	7.37
plot C, High polymer concentration - Low Flow rate	71.5	78.2	73.94	2.99
plot D , High polymer concentration & Flow rate	75.5	87	83.8	5.6

Polymer concentration ratio Levels= Low (4-6.4), High (6.5-9), Flow rate (ml/h) Levels= Low (0.5-0.99 ml/h), High (1-1.5 ml/h),

chitosan/PEO concentration on nanofiber diameter was similar to the previous data (both of these parameters reversely related with fibers diameter). As shown in 3D plots, the relationship between the distance and fibers size was the same as the results in Fig. 9, while the flow rate and the fibers diameter did not show a constant relation.

Totally, chitosan is difficult to synthesize electrospun nanofibers due to its high surface tension and high viscosity in solution because of the production of beaded and short noncontinues fibers. To overcome these difficulties, chitosan can be blended with the PEO to produce free-beaded nanofibers. This study exhibits that input variables, including in electrospinning such as chitosan/PEO concentration ratio, applied voltage, flow rate, and distance between nozzle tip and collector, have considerable effect on nanofiber diameter. The results indicate that the most effect depends on chitosan/PEO concentration; however, the interactions between the other parameters affect the fibers diameter.

4 Conclusion

In this study, the ANN model was designed to predict electrospun chitosan/PEO nanofiber diameter using four variables, including chitosan/PEO concentration ratio, applied voltage, flow rate, and distance between nozzle tip and collector. The results indicated that the designed ANN predicts diameter of chitosan/PEO nanofibers with MSE and regression coefficient, and the correlation between the diameter of observed and predicted fibers is significant. The most effect depends on chitosan/PEO concentration; however, the effect of interaction between other parameters affects the fibers diameter. Therefore, the ANN model suits for predicting diameter of chitosan/PEO nanofibers in trials and studies. The best results were obtained via network with three hidden layers including 10, 15, and 5 nodes in each layer, respectively, and the mean square error (MSE) and correlation coefficient between the observed and predicted thickness of the nanofibers in the chosen model were

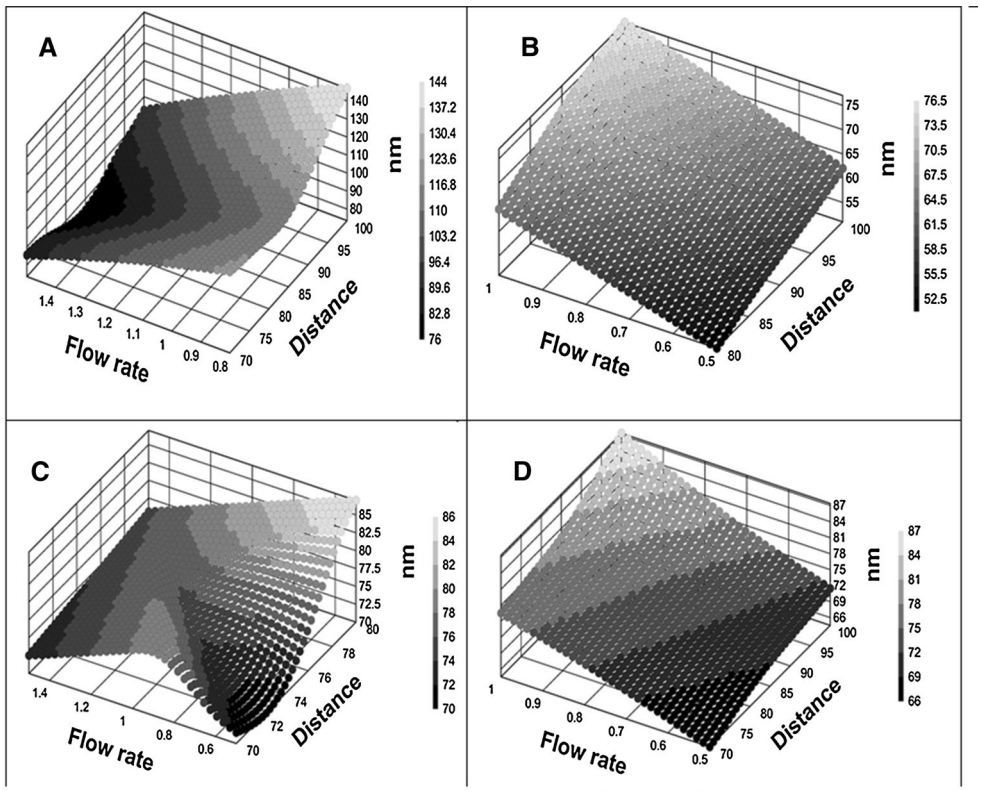

Fig. 10 3D plots of flow rate–nozzle-to-collector distance, and data of nanofiber diameter modeling via ANN in different polymer concentration and applied voltage levels

Diagrams \ Nanofibers diameter (Z) Data	Minimum Z (nm)	Maximum Z (nm)	Mean (nm)	Standard deviation
plot A, Low polymer concentration & applied voltage levels	79	132.7	109.17	22.29
plot B , Low polymer concentration -High applied voltage	51	72	62.4	8.70
plot C, High polymer concentration -Low applied voltage	71.5	78.2	74.45	3.04
plot D , High polymer concentration & applied voltage	72	78.5	75.55	2.85

Polymer concentration ratio Levels= Low (4-6.4), High (6.5-9), Applied voltage Levels= Low (20-22.9 kV), High (23-26.5 kV),

about 0.0707 and 0.9630, respectively. In addition, applying a mix of two kinds of others solutions and polymers, and evaluating other variables can have a better understanding for the determination of electrospun nanofiber diameter using ANN technique.

Acknowledgments This project was supported by Tehran University of Medical Sciences (TUMS), Grant No. 93-04-87-27607.

References

1. Ma Z, Kotaki M, Inai R, Ramakrishna S (2005) Potential of nanofiber matrix as tissue-engineering scaffolds. Tissue Eng 11(1–2):101–109
2. Fang J, Wang X, Lin T (2011) Functional applications of electrospun nanofibers. In: Tong L (ed) Nanofibers-production, properties and functional applications. InTech–Open Access Publisher, Rijeka, Croatia, pp 287–326
3. Huang Z-M, Zhang YZ, Kotaki M, Ramakrishna S (2003) A review on polymer nanofibers by electrospinning and their applications in nanocomposites. Compos Sci Technol 63(15):2223–2253
4. Deitzel JM, Kleinmeyer J, Harris DEA, Tan NCB (2001) The effect of processing variables on the morphology of electrospun nanofibers and textiles. Polymer 42(1):261–272
5. Agarwal S, Wendorff JH, Greiner A (2008) Use of electrospinning technique for biomedical applications. Polymer 49(26):5603–5621
6. Beachley V, Wen X (2009) Effect of electrospinning parameters on the nanofiber diameter and length. Mater Sci Eng C 29(3):663–668
7. Maleki M, Amani-Tehran M, Latifi M, Mathur S (2014) Drug release profile in core–shell nanofibrous structures: a study on Peppas equation and artificial neural network modeling. Comput Meth Prog Bio 113(1):92–100
8. Ziabari M, Mottaghitalab V, Haghi AK (2009) Application of direct tracking method for measuring electrospun nanofiber diameter. Braz J Chem Eng 26(1):53–62
9. Gibson PW, Lee C, Ko F, Reneker D (2007) Application of nanofiber technology to nonwoven thermal insulation. J Eng Fiber Fabr 2(2):32–40
10. Pham QP, Sharma U, Mikos AG (2006) Electrospinning of polymeric nanofibers for tissue engineering applications: a review. Tissue Eng 12(5):1197–1211
11. Naghibzadeh M, Adabi M (2014) Evaluation of effective electrospinning parameters controlling gelatin nanofibers diameter via modelling artificial neural networks. Fiber Polym 15(4):767–777

12. Ribeiro C, Sencadas V, Ribelles JLG, Lanceros-Méndez S (2010) Influence of processing conditions on polymorphism and nanofiber morphology of electroactive poly (vinylidene fluoride) electrospun membranes. Soft Mater 8(3):274–287
13. Rošic R, Pelipenko J, Kocbek P, Baumgartner S, Bešter-Rogač M, Kristl J (2012) The role of rheology of polymer solutions in predicting nanofiber formation by electrospinning. Eur Polym J 48(8):1374–1384
14. Yördem OS, Papila M, Menceloğlu YZ (2008) Effects of electrospinning parameters on polyacrylonitrile nanofiber diameter: an investigation by response surface methodology. Mater Des 29(1):34–44
15. Vasita R, Katti DS (2006) Nanofibers and their applications in tissue engineering. Int J Nanomed 1(1):15
16. Gibson P, Schreuder-Gibson H, Rivin D (2001) Transport properties of porous membranes based on electrospun nanofibers. Colloids Surf A 187:469–481
17. Khanlou HM, Sadollah A, Ang BC, Kim JH, Talebian S, Ghadimi A (2014) Prediction and optimization of electrospinning parameters for polymethyl methacrylate nanofiber fabrication using response surface methodology and artificial neural networks. Neural Comput Appl 25(3–4):767–777
18. Qu J, Wang D, Wang H, Dong Y, Zhang F, Zuo B, Zhang H (2013) Electrospun silk fibroin nanofibers in different diameters support neurite outgrowth and promote astrocyte migration. J Biomed Mater Res A 101(9):2667–2678
19. Kanafchian M, Valizadeh M, Haghi AK (2011) Prediction of nanofiber diameter for improvements in incorporation of multilayer electrospun nanofibers. Korean J Chem Eng 28(3):751–755
20. Thompson CJ, Chase GG, Yarin AL, Reneker DH (2007) Effects of parameters on nanofiber diameter determined from electrospinning model. Polymer 48(23):6913–6922
21. Faridi-Majidi R, Ziyadi H, Naderi N, Amani A (2012) Use of artificial neural networks to determine parameters controlling the nanofibers diameter in electrospinning of nylon-6, 6. J Appl Polym Sci 124(2):1589–1597
22. Nasouri K, Bahrambeygi H, Rabbi A, Shoushtari AM, Kaflou A (2012) Modeling and optimization of electrospun PAN nanofiber diameter using response surface methodology and artificial neural networks. J Appl Polym Sci 126(1):127–135
23. Rezaei B, Askari M, Shoushtari AM, Ghani M, Haji A (2012) Application of response surface methodology (RSM) and Artificial Neural Network (ANN) in diameter optimization of thermo regulating nanofibers
24. Nasouri K, Shoushtari AM, Khamforoush M (2013) Comparison between artificial neural network and response surface methodology in the prediction of the production rate of polyacrylonitrile electrospun nanofibers. Fiber Polym 14(11):1849–1856
25. Rabbi A, Nasouri K, Bahrambeygi H, Shoushtari AM, Babaei MR (2012) RSM and ANN approaches for modeling and optimizing of electrospun polyurethane nanofibers morphology. Fiber Polym 13(8):1007–1014
26. Desai KM, Survase SA, Saudagar PS, Lele SS, Singhal RS (2008) Comparison of artificial neural network (ANN) and response surface methodology (RSM) in fermentation media optimization: case study of fermentative production of scleroglucan. Biochem Eng J 41(3):266–273
27. Bas D, Boyaci IH (2007) Modeling and optimization II: comparison of estimation capabilities of response surface methodology with artificial neural networks in a biochemical reaction. J Food Eng 78(3):846–854
28. Lou W, Nakai S (2001) Application of artificial neural networks for predicting the thermal inactivation of bacteria: a combined effect of temperature, pH and water activity. Food Res Int 34(7):573–579
29. Marchitan N, Cojocaru C, Mereuta A, Duca G, Cretescu I, Gonta M (2010) Modeling and optimization of tartaric acid reactive extraction from aqueous solutions: a comparison between response surface methodology and artificial neural network. Sep Purif Technol 75(3):273–285
30. Montgomery DC, Myers RH (1995) Response surface methodology: process and product optimization using designed experiments. Raymond H Meyers and Douglas C Montgomery A Wiley-Interscience Publications
31. Datt G (2012) An evolutionary approach: analysis of artificial neural networks. Int J Emerg Technol Adv Eng 2(1):160–164
32. Jha GK (2007) Artificial neural networks. Indian Agricultural Research Institute, New Delhi
33. Abraham A (2005) Artificial neural networks. In: Sydenham P, Thorn R (eds) Handbook of measuring system design. Wiley, pp 901–908
34. Yadav JS, Yadav M, Jain A (2014) Artificial neural network. Int J Sci Res Educ 1(06):108–118
35. Tu JV (1996) Advantages and disadvantages of using artificial neural networks versus logistic regression for predicting medical outcomes. J Clin Epidemiol 49(11):1225–1231
36. Aghajani M, Shahverdi AR, Rezayat SM, Amini MA, Amani A (2013) Preparation and optimization of acetaminophen nanosuspension through nanoprecipitation using microfluidic devices: an artificial neural networks study. Pharm Dev Technol 18(3):609–618
37. Chen XK (2014) Prediction of tensile properties of CNF/epoxy composites using artificial neural network. Trans Tech Publ 898:111–114
38. Adabi M, Saber R, Naghibzadeh M, Faridbod F, Faridi-Majidi R (2015) Parameters affecting carbon nanofiber electrodes for measurement of cathodic current in electrochemical sensors: an investigation using artificial neural network. RSC Adv 5(99):81243–81252
39. Kang YO, Yoon IS, Lee SY, Kim DD, Lee SJ, Park WH, Hudson SM (2010) Chitosan-coated poly (vinyl alcohol) nanofibers for wound dressings. J Biomed Mater Res B 92(2):568–576
40. Geng X, Kwon O-H, Jang J (2005) Electrospinning of chitosan dissolved in concentrated acetic acid solution. Biomaterials 26(27):5427–5432
41. Sun K, Li ZH (2011) Preparations, properties and applications of chitosan based nanofibers fabricated by electrospinning. Express Polym Lett 5(4):342–361
42. Karimi MA, Pourhakkak P, Adabi M, Firoozi S, Adabi M, Naghibzadeh M (2015) Using an artificial neural network for the evaluation of the parameters controlling PVA/chitosan electrospun nanofibers diameter. e-Polymers 15(2):127–138
43. Talebi R, Ghiasi MM, Talebi H, Mohammadyian M, Zendehboudi S, Arabloo M, Bahadori A (2014) Application of soft computing approaches for modeling saturation pressure of reservoir oils. J Nat Gas Sci Eng 20:8–15
44. Esnaashari SS, Rezaei S, Mirzaei E, Afshari H, Rezayat SM, Faridi-Majidi R (2014) Preparation and characterization of kefiran electrospun nanofibers. Int J Biol Macromol 70:50–56
45. Jia Y-T, Gong J, Gu X-H, Kim H-Y, Dong J, Shen X-Y (2007) Fabrication and characterization of poly (vinyl alcohol)/chitosan blend nanofibers produced by electrospinning method. Carbohyd Polym 67(3):403–409
46. Adabi M, Saber R, Faridi-Majidi R, Faridbod F (2015) Performance of electrodes synthesized with polyacrylonitrile-based carbon nanofibers for application in electrochemical sensors and biosensors. Mater Sci Eng, C 48:673–678